

# Crosslinking by Etherification of Bisepoxide with Divalent Metal Salts of *p*-Aminobenzoic Acid

SHIGETOSHI TAKECHI and HIDEAKI MATSUDA\*

Research Laboratory, Okura Industrial Co., Ltd., 1515 Nakatsu-cho, Marugame, Kagawa-ken 763, Japan

## SYNOPSIS

Crosslinking by etherification of a large excess of bisepoxide with divalent metal salts of *p*-aminobenzoic acid was investigated. Mg and Ca were selected as the divalent metal salts, and bisphenol A diglycidyl ether was the bisepoxide used. In the crosslinking reactions, the metal salts exhibited catalytic activity for the etherification, with the Ca salt showing higher catalytic activity than the Mg salt. Hence, the etherification proceeded via an ionic mechanism in which carboxylate anion is concerned. The orders of reaction with respect to carboxylate anion concentration were one order for the both systems. The overall activation energies of the crosslinking reaction were 13.4 kcal/mol for the system containing Mg and 23.0 kcal/mol for the system containing Ca. The metal-containing cured resins obtained showed higher flexural strength, Rockwell hardness, and compressive strength than the resins without metal. Heat distortion temperature and glass transition temperature determined by dynamic mechanical properties increased with an increase in the metal salt content in the feed. Thermal decomposition was accelerated by the incorporated metal. In addition, the metal-containing cured resins have high boiling water and water resistances.

© 1994 John Wiley & Sons, Inc.

## INTRODUCTION

Divalent metal salts of *p*-aminobenzoic acid (ABA), that is, ABA(M) (where M is a divalent metal such as Mg or Ca) are of interest from scientific and industrial standpoints because the salts have an ionic bond formed between  $\text{—COO}^-$  and  $\text{M}^{2+}$ , and two amino groups. We have been active in the syntheses of ionic polymers by using the ABA(M) salts.<sup>1-4</sup>



M = divalent metal (Mg or Ca)

Previously, crosslinking of bisepoxide with ABA(M) and aromatic diamine was investigated.<sup>3</sup> As the bisepoxide, bisphenol A diglycidyl ether

(BADG) was used. 4,4'-Diaminodiphenylmethane (4,4'-methylenedianiline (MDA) was used as the aromatic diamine. It was found that the metal carboxylate groups in ABA(M) catalyzed the crosslinking reaction. In this case, the salt containing Ca with the lower electronegativity showed higher catalytic activities than the Mg salt. Hence, the crosslinking reaction proceeded via an ionic mechanism. Further, the metal carboxylate groups in ABA(M) were also found to have catalytic activity for etherification of epoxy group as a side reaction. It seemed of interest to prepare novel metal-containing cured resins by etherification of epoxy groups of BADG by the catalytic action of the metal carboxylate groups in ABA(M).

Therefore, in the present study, crosslinking of curable mixtures prepared from ABA(M) and a large excess of BADG was investigated by taking advantage of the catalytic activity of ABA(M) for the etherification of epoxy groups. The novel metal-containing cured resins obtained were evaluated for physical and other properties.

\* To whom correspondence should be addressed.

Journal of Applied Polymer Science, Vol. 54, 1977-1988 (1994)

© 1994 John Wiley & Sons, Inc.

CCC 0021-8995/94/121977-12

## EXPERIMENTAL

### Materials

The ABA(M) salts were prepared by the same method as reported previously.<sup>1</sup> As the BADG, EPOMIK R139 (Mitsui Petrochemical Epoxy Co.) was used. The epoxy value was 5.478 equiv/kg (calcd. = 5.875 equiv/kg). MDA, *N,N*-dimethylformamide (DMF), and *N,N*-dimethylbenzylamine (DMBA) were of specialty grade and were used as received.

### Curing Reactions

The typical example was as follows: A fixed amount of ABA(M) was dissolved in a given amount of DMF, then a given amount of BADG was added. The solution thus obtained was heated at 100°C for 1 h and the DMF was completely removed under a reduced pressure at 100°C to obtain a homogeneous, curable mixture. Next, 5 g of the curable mixture was placed in an 18 × 180 mm test tube and the tube was placed in a fixed temperature bath. After a desired time, samples were taken for analysis of epoxy values. Gel time was determined by measuring the time at which the mixture would not flow in the test tube.

Cured resin moldings for determining physical and other properties were prepared as follows: A desired amount of the above curable mixture was degassed under a reduced pressure and poured into molds. The mixture was cured at 120°C for 24 h, 150°C for 16 h, and then 180°C for 5 h. Since mixtures containing MDA as an aromatic amine do not cure, DMBA (2.0 wt % based on the total weight of the mixture) was added as a catalyst.

### Determination of Order of Reaction with Respect to [—COO<sup>-</sup>]

For the systems of ABA(M)-MDA-BADG, the overall rate ( $V_a$ ) of crosslinking reaction is expressed as

$$V_a = k[\text{—OH}]^1[\text{Ep}]^m[\text{—COO}^-]^n \quad (1)$$

Here,  $k$  is the overall rate constant; [—OH], [Ep], and [—COO<sup>-</sup>] are the concentrations of hydroxyl group, epoxy group, and carboxylate group in the reaction system, respectively.

In the initial stage of the crosslinking reaction, [—OH] and [Ep] are considered to be nearly constant, hence, eq. (1) can be written as follows:

$$V_a = K[\text{—COO}^-]^n$$

$$(K = k[\text{—OH}]^1[\text{Ep}]^m : K \text{ is a constant}) \quad (2)$$

By rearranging, eq. (2) can be expressed by the following:

$$\ln V_a = n \ln[\text{—COO}^-] + \ln K \quad (3)$$

Therefore,  $V_a$  was determined by measuring [Ep] in the initial stage of the crosslinking reaction for the systems with various [—COO<sup>-</sup>], and  $\ln V_a$  were plotted against  $\ln[\text{—COO}^-]$ . The order of reaction with respect to [—COO<sup>-</sup>] was calculated from the slope obtained from the least-squares fits of the plots.

### Determination of Overall Activation Energies of Crosslinking Reactions

[—COO<sup>-</sup>] is constant for the system of ABA(M)-BADG at the same mole ratio, and [—OH] and [Ep] are nearly constant in the initial stage of the crosslinking reaction. Therefore, eq. (1) can be written as

$$V_a = kC \quad (C = [\text{—OH}]^1[\text{Ep}]^m[\text{—COO}^-]^n : C \text{ is constant}) \quad (4)$$

By rearranging eq. (4), we get

$$k = V_a/C \quad (5)$$

Introducing eq. (5) into Arrhenius' equation, we get

$$\ln V_a = -E_a/RT + \ln AC \quad (6)$$

Here,  $E_a$  is the overall activation energy of the crosslinking reaction;  $R$ ,  $T$ , and  $A$  are the gas constant, the reaction temperature, and the frequency factor, respectively.  $V_a$  was determined for various temperatures. Based on this relationship, the  $E_a$  were calculated from the slope obtained from the least-squares fits of the plots.

### Analytical Methods

When a sample was an insoluble hard solid, it was filed into powder and subjected to analysis. The titrations were carried out by using a Hiranuma reporting titrater (COMMIT 101).



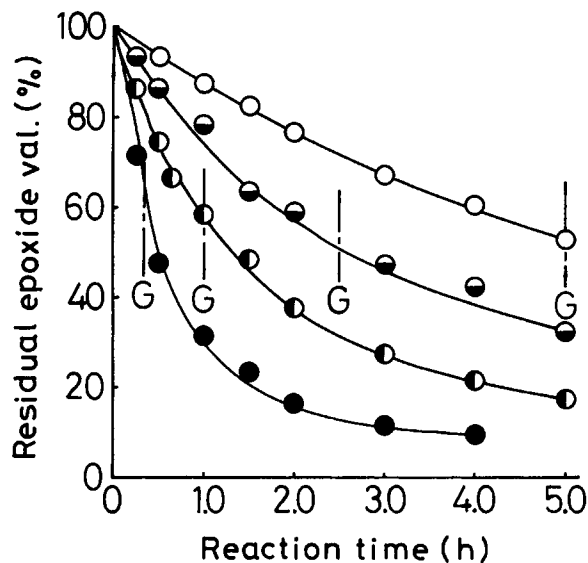


**Figure 2** Curing reactions of ABA(Ca)-MDA-BADG systems at 150°C: (●) ABA(Ca)-BADG (1 : 20); (◐) ABA(Ca)-MDA-BADG (0.5 : 0.5 : 20); (◑) ABA(Ca)-MDA-BADG (0.3 : 0.7 : 20); (○) ABA(Ca)-MDA-BADG (0.15 : 0.85 : 20). *G* = gel point.

eq. (3). The relationships between  $\ln [-\text{COO}^-]$  and  $\ln V_a$ , which were determined from the slope of the straight part in the initial stage of the curing reaction

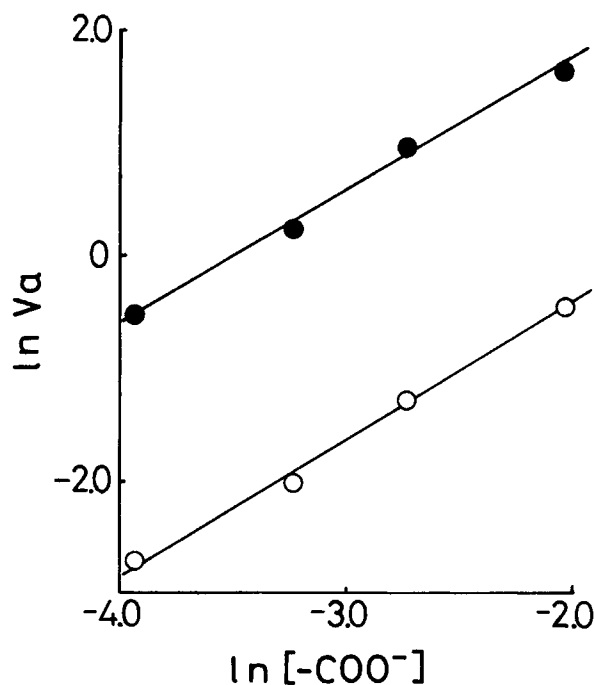


**Figure 3** Relationship between  $[-\text{COO}^-]$  and reaction rate ( $V_a$ ) for metal-containing systems at 150°C: (○) Mg-containing systems; (●) Ca-containing systems.

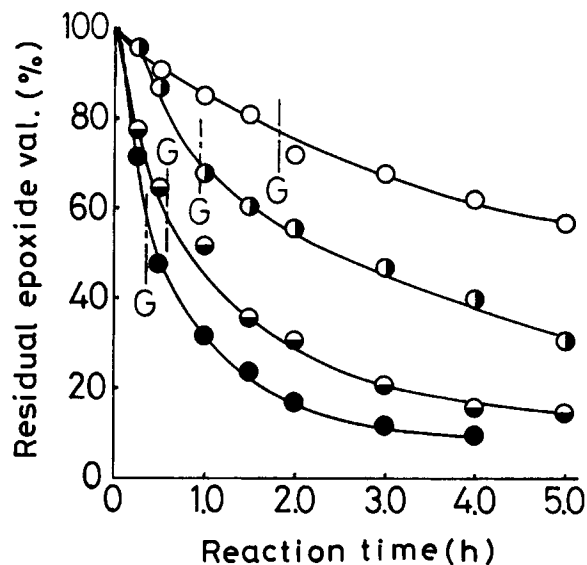


**Figure 4** Effect of reaction temperature on curing reactions of ABA(Ca)-BADG (1 : 20) system: (○) 120°C; (◐) 130°C; (◑) 140°C; (●) 150°C. *G* = gel point.

in Figure 2, are shown in Figure 3. Plots of  $\ln [-\text{COO}^-]$  vs.  $\ln V_a$  gave straight lines with a slope of 1.1 as the order of reaction with respect to  $[-\text{COO}^-]$  for the ABA(Ca)-BADG system, and with a slope of 1.2 for the ABA(Mg)-BADG system. These results suggest the participation of one  $-\text{COO}^-$  group in the curing reactions.

Figure 4 exhibits the curing reactions of the

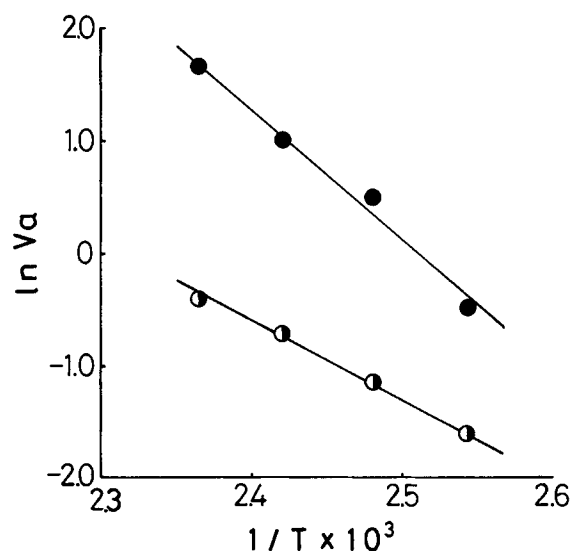


**Figure 5** Arrhenius plots of curing reactions of ABA(M)-BADG (1 : 20) systems: (●) ABA(Mg); (○) ABA(Ca).

**Table I** Cure Properties<sup>a</sup> of ABA(M)-BADG and MDA-BADG Systems

| Components            | Mole Ratio of Components | Metal Content (%) (Calcd.) | Gel Time (min) | Final Conversion of Epoxide (%) |
|-----------------------|--------------------------|----------------------------|----------------|---------------------------------|
| MDA-BADG <sup>b</sup> | 1 : 40                   | —                          | 91             | 99                              |
|                       | 1 : 20                   | —                          | 43             | 99                              |
|                       | 1 : 13.3                 | —                          | 29             | 100                             |
|                       | 1 : 10                   | —                          | 9              | 99                              |
| ABA (Mg)-BADG         | 1 : 40                   | 0.16                       | > 500          | 97                              |
|                       | 1 : 20                   | 0.32                       | 300            | 95                              |
|                       | 1 : 13.3                 | 0.47                       | 36             | 94                              |
|                       | 1 : 10                   | 0.62                       | 14             | 93                              |
| ABA (Ca)-BADG         | 1 : 40                   | 0.27                       | 101            | 99                              |
|                       | 1 : 20                   | 0.53                       | 20             | 98                              |
|                       | 1 : 13.3                 | 0.77                       | 12             | 96                              |
|                       | 1 : 10                   | 1.01                       | 6              | 95                              |

<sup>a</sup> Cure condition = 120°C, 24 h; 150°C, 16 h; and 180°C, 5 h. Gel time was determined at 150°C.

<sup>b</sup> DMBA was added as a catalyst at a concentration of 2.0 wt % based on the total weight of reactants.

ABA(Ca)-BADG (1 : 20) system at 120°C ~ 150°C. The gelation times were 110 min at 120°C, 55 min at 130°C, 35 min at 140°C, and 20 min at 150°C, respectively. A similar tendency was obtained for the ABA(Mg)-BADG (1 : 20) system. The relationships between  $1/T$  and  $\ln V_a$ , which were determined from the slope of the straight part in the initial stage of the curing reactions in Figure 4, are shown in Figure 5. According to eq. (6), the overall activation energies  $E_a$  were calculated as follows: 13.4 kcal/mol for the ABA(Mg)-BADG (1 : 20) system and 23.0 kcal/mol for the ABA(Ca)-BADG (1 : 20) system.

Table I shows the cure properties of various systems. The gelation time of these systems at 150°C decreased with increase in the metal content, and that of the ABA(Ca)-BADG (1 : 10) system at 150°C was very short: 6 min. The gelation time of the MDA-BADG systems containing DMBA as a catalyst decreased with increase in the MDA content, although the systems contained the same concentration of DMBA. The amount of hydroxyl groups in the system is considered to increase with increase in the MDA content. Therefore, it is suggested that the hydroxyl groups accelerate the etherification of epoxy groups. Final conversions of epoxy groups after curing at 120°C for 24 h, 150°C for 16 h, and 180°C for 5 h were above 93% for all the systems.

Figures 6 and 7 show the IR spectra of the MDA-BADG (1 : 20) system and the ABA(Ca)-BADG (1 : 20) system, respectively. The absorption band at ca. 900  $\text{cm}^{-1}$  due to the epoxy group is noteworthy in the spectra before curing. On the other hand, in the spectra after the curing, this band has disappeared and the band of the ether linkage at ca. 1100

$\text{cm}^{-1}$  has increased, showing that the crosslinking reaction by etherification of epoxy groups has fully proceeded. Further, for the metal-containing system, the small band at ca. 1400  $\text{cm}^{-1}$  in the spectrum of the initial curable mixture is attributable to the carboxylate group.

In the spectrum of the metal-containing system before the curing, there is a large absorption band at ca. 1700  $\text{cm}^{-1}$ . However, this band has almost disappeared from the spectrum after the curing and is not observed in the spectra before and after the curing of the MDA-BADG (1 : 20) system not containing metal. The ABA(M) salts contain carbonyl groups, however the band due to the carbonyl group appears at ca. 1600  $\text{cm}^{-1}$ . From this, the band at ca. 1700  $\text{cm}^{-1}$  is not attributable to ABA(M). In addition, the band at ca. 1650  $\text{cm}^{-1}$  due to the carbonyl group of DMF is not found in the spectra before the curing, indicating that there is no residual DMF.

Price and Carmelite<sup>5</sup> reported that oligomers having allyl group were formed by etherification of propyleneoxide catalyzed by potassium-*t*-butoxide in dimethylsulfoxide. Similarly, Tanaka et al.<sup>6</sup> studied etherification of phenylglycidylether (PGE) catalyzed by DMBA in the presence of *n*-butanol. In this case, they found the following facts. There is an induction period in the initial stage of the etherification, and the rate of etherification follows  $-d[\text{PGE}]/dt = k_1[\text{PGE}][\text{DMBA}]$ . The products are oligomers of PGE. The oligomers contain many phenylvinylether group  $\text{C}_6\text{H}_5-\text{O}-\text{CH}=\text{CHCH}_2\text{O}-$ , and the etherification is accelerated by addition of alcohols. From these results, the following reaction schemes were given:

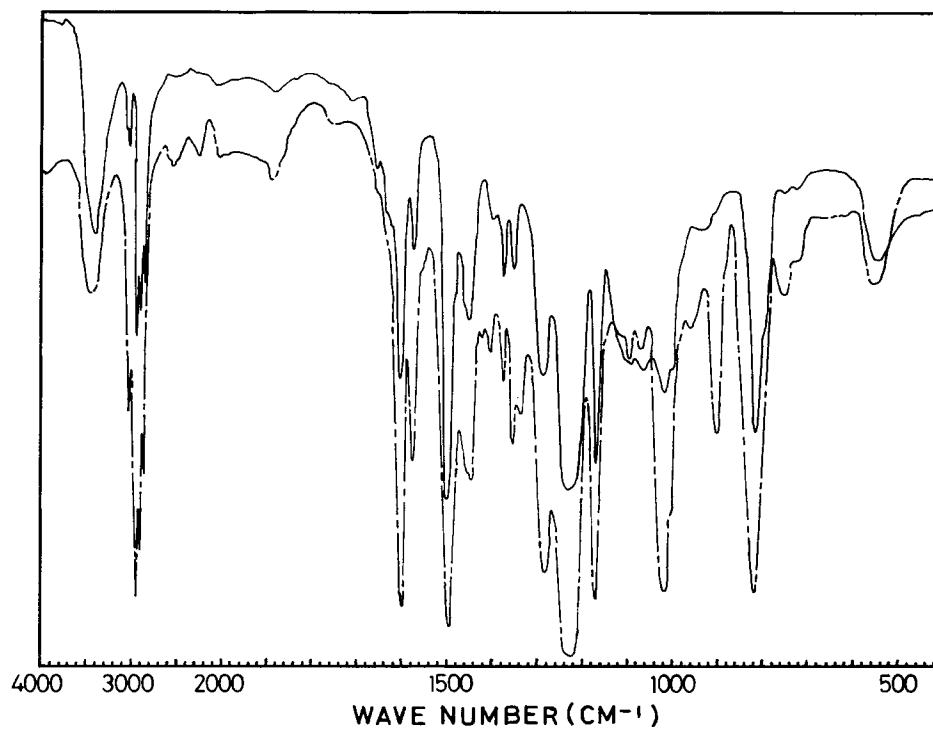


**Figure 6** Infrared spectra of MDA-BADG (1 : 20) system: (---) initial curable mixture; (—) cured at 120°C for 24 h, at 150°C for 16 h, and at 180°C for 5 h.

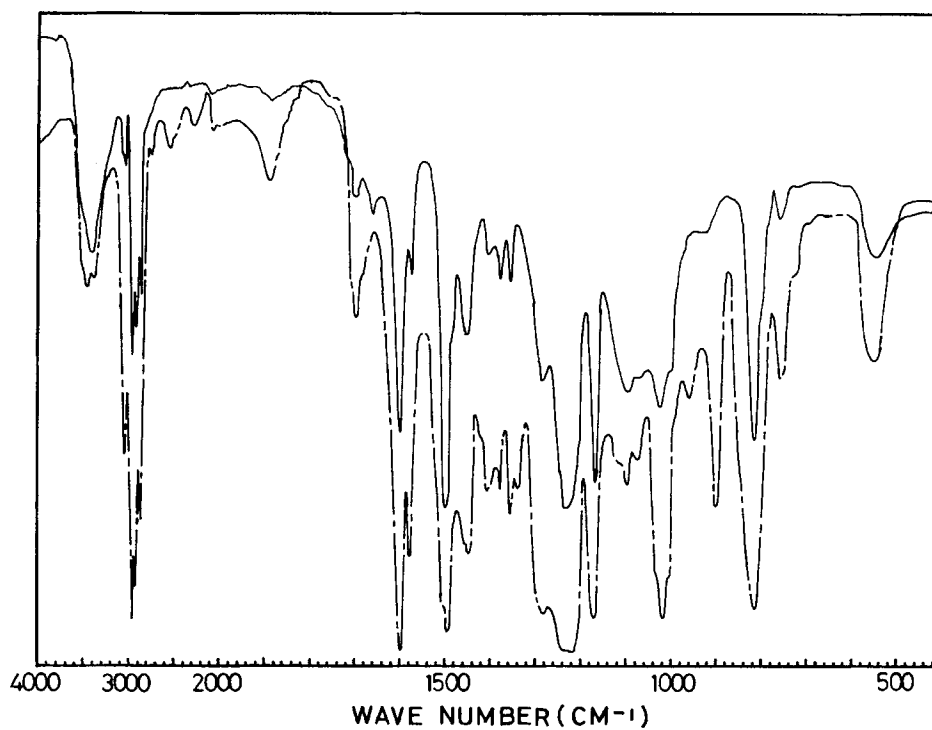
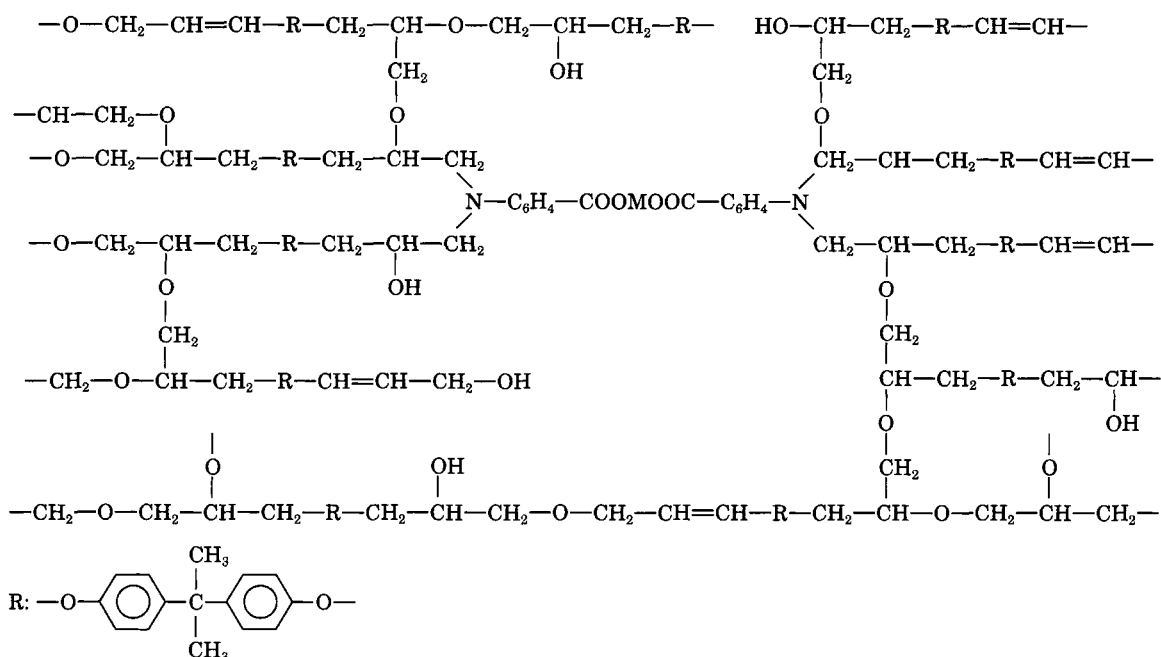


**Figure 7** Infrared spectra of ABA(Ca)-BADG (1 : 20) system: (---) initial curable mixture; (—) cured at 120°C for 24 h, at 150°C for 16 h, and at 180°C for 5 h.



Of the above reactions, the reaction shown by eq. (16) results in an extension of the molecular chains, while crosslinking reactions are shown by eqs. (13) and (18). Therefore, as the reactions of eq. (13) and

(18) occur, the crosslinking density increases. The idealized main structure part of the novel metal-containing cured resins obtained in the present study may be represented as follows:



### Physical Properties

Table II shows the physical properties of the cured resins. The heat distortion temperature (HDT) increased with increase in the aromatic amine content in the feed, and the MDA-containing cured resins exhibited higher values than the metal-containing

cured resins at the same mole ratios. It is suggested that the crosslinking densities of the cured resins are affected by the mole ratios of the components and the species of catalysts. That is, the rate of reaction of MDA or ABA(M) with epoxy groups as shown by eqs. (7) and (8) was faster than that of the etherification of epoxy groups. The tertiary

**Table II.** Physical Properties of Cured Resins

| Components            | Mole Ratio of Components | HDT (°C) | Tensile Strength (kg/cm <sup>2</sup> ) | Flexural Strength (kg/cm <sup>2</sup> ) | Rockwell Hardness (M Scale) | Impact Strength (kg·cm/cm) | Compressive Strength (kg/cm <sup>2</sup> ) |
|-----------------------|--------------------------|----------|--|---|-----------------------------|----------------------------|--|
| MDA-BADG <sup>a</sup> | 1 : 40                   | 109      | 680                                    | 1170                                    | 98                          | 1.21                       | 1350                                       |
|                       | 1 : 20                   | 101      | 630                                    | 1100                                    | 105                         | 1.06                       | 1400                                       |
|                       | 1 : 13.3                 | 123      | 620                                    | 1180                                    | 103                         | 1.34                       | 1370                                       |
|                       | 1 : 10                   | 140      | 530                                    | 1030                                    | 104                         | 1.18                       | 1460                                       |
| ABA (Mg)-BADG         | 1 : 40                   | 95       | 800                                    | 1290                                    | 101                         | 1.34                       | 1430                                       |
|                       | 1 : 20                   | 103      | 760                                    | 1310                                    | 108                         | 1.46                       | 1550                                       |
|                       | 1 : 13.3                 | 116      | 480                                    | 1260                                    | 112                         | 1.16                       | 1530                                       |
|                       | 1 : 10                   | 118      | 640                                    | 1120                                    | 112                         | 1.06                       | 1620                                       |
| ABA (Ca)-BADG         | 1 : 40                   | 105      | 670                                    | 1270                                    | 108                         | 1.17                       | 1420                                       |
|                       | 1 : 20                   | 102      | 690                                    | 1200                                    | 110                         | 1.27                       | 1520                                       |
|                       | 1 : 13.3                 | 110      | 540                                    | 1210                                    | 114                         | 0.98                       | 1600                                       |

<sup>a</sup> DMBA was added as a catalyst at a concentration of 2.0 wt % based on the total weight of reactants.



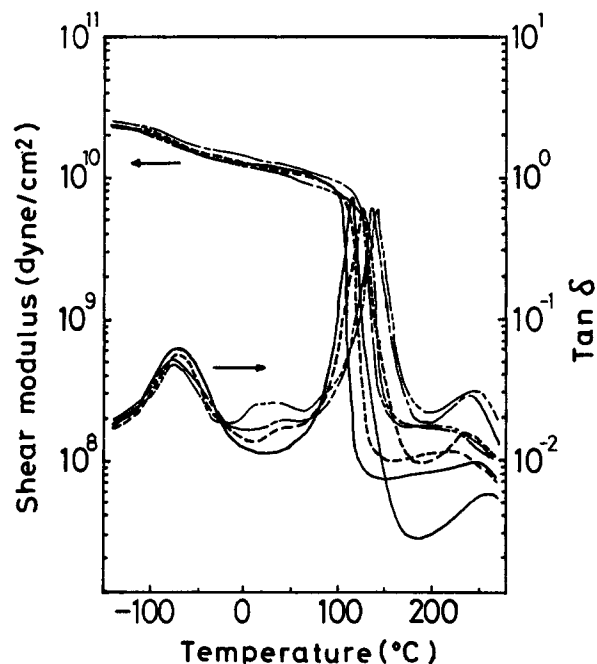


**Figure 8** Dynamic mechanical properties of cured resins. (—) ABA(Mg)-BADG (1 : 40); (-----) ABA(Mg)-BADG (1 : 20); (- - -) ABA(Mg)-BADG (1 : 13.3); (----) ABA(Mg)-BADG (1 : 10).

amine groups produced by the reactions of the primary amines with two epoxy groups are considered to act as crosslinking points in the cured resins. With increase in the aromatic amine content in the system, the concentration of hydroxyl groups produced by the reactions of amino groups with epoxy groups in the preparation of curable mixture increases; hence, the degree of occurrence of the reactions as

shown by eq. (13) would become high, leading to high crosslinking densities of the cured resin.

As previously stated, Tanaka et al.<sup>6</sup> reported that polymerization of PGE catalyzed by DMBA gave oligomers whose molecular weights were only several hundreds. In the present study, the termination reaction as shown by eq. (17) is considered to occur after several epoxy groups add to the hydroxyl group produced by eqs. (7) and (8) [eqs. (13), and (18)]. Systems with small aromatic amine content show many epoxy groups before curing, and part of them is presumed to form the intermediate as shown by eq. (14), followed by the reaction of eq. (16), which does not produce a crosslinking point. This might be the reason why the systems with small aromatic amine content gave cured resins with low crosslinking densities.

In the ABA(M)-BADG systems, it is guessed that the reactions of eq. (16) and/or eqs. (15) and (17) occur more frequently than in the MDA-BADG systems, resulting in lower crosslinking densities of the metal-containing cured resins. This might be the cause of the lower HDT of the metal-containing cured resins, compared with the HDT of the cured resins based on MDA.

The tensile and flexural strengths showed a tendency to decrease with increase in the aromatic amine content in the feed. However, the reverse trend was observed for Rockwell hardness and compressive strength. Further, the ABA(M)-BADG cured resins exhibited higher flexural and compressive strengths, and higher Rockwell hardness than the MDA-BADG cured resins. Thus, the effect of introducing metal appears in this case.

**Table III** Dynamic Mechanical Properties of Cured Resins

| Components            | Mole Ratio of Components | $\alpha$ -Transition Temp. (°C) | $\beta$ -Transition |                    |
|-----------------------|--------------------------|---------------------------------|---------------------|--------------------|
|                       |                          |                                 | Temp. (°C)          | Tan $\delta_{max}$ |
| MDA-BADG <sup>a</sup> | 1 : 40                   | 117                             | -75                 | 0.053              |
|                       | 1 : 20                   | 119                             | -66                 | 0.055              |
|                       | 1 : 13.3                 | 136                             | -72                 | 0.054              |
|                       | 1 : 10                   | 158                             | -68                 | 0.055              |
| ABA (Mg)-BADG         | 1 : 40                   | 111                             | -71                 | 0.057              |
|                       | 1 : 20                   | 124                             | -70                 | 0.055              |
|                       | 1 : 13.3                 | 137                             | -75                 | 0.052              |
|                       | 1 : 10                   | 139                             | -76                 | 0.049              |
| ABA (Ca)-BADG         | 1 : 40                   | 124                             | -69                 | 0.049              |
|                       | 1 : 20                   | 123                             | -71                 | 0.050              |
|                       | 1 : 13.3                 | 130                             | -73                 | 0.049              |
|                       | 1 : 10                   | 136                             | -74                 | 0.049              |

<sup>a</sup> DMBA was added as a catalyst at a concentration of 2.0 wt % based on the total weight of reactants.

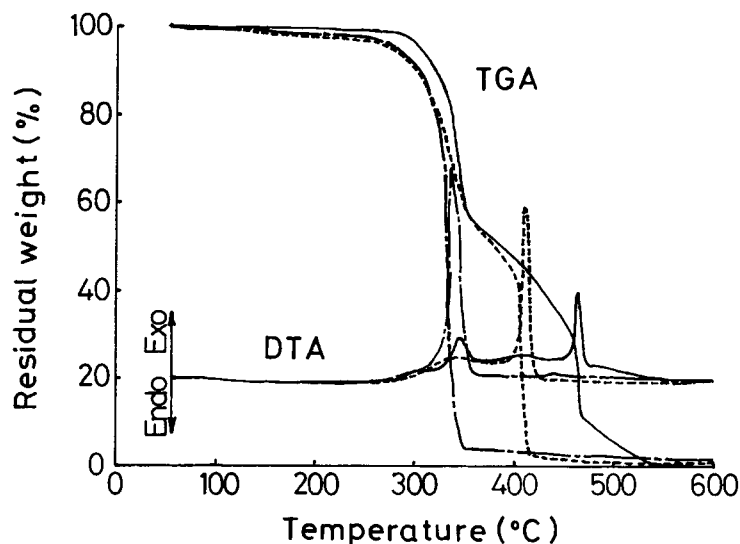


**Figure 9** TGA and DTA curves of cured resins. (—) MDA-BADG (1 : 10); (-----) ABA(Mg)-BADG (1 : 10); (- - -) ABA(Ca)-BADG (1 : 10).

### Dynamic Mechanical Properties

Figure 8 shows the dynamic mechanical properties of the cured resins. They exhibited relaxations at ca. 110° ~ 140°C and -70°C. These will be denoted by  $\alpha$  and  $\beta$  relaxations, respectively. Further, the cured resins which contained a large amount of ABA(Mg) exhibited a small relaxation at room temperature. This will be denoted by  $\beta'$  relaxation. Since the measurements were conducted at small frequencies below 3.0 Hz, a temperature at which shear modulus (G) suddenly decreases or  $\tan \delta$  shows the major maximum is considered to be glass transition temperature ( $T_g$ ).

The  $\tan \delta$  showed a sharp peak and the G suddenly decreased at the  $\alpha$  relaxation, hence, the  $\alpha$  relaxation is considered to be  $T_g$ . The plateaus observed for G above  $T_g$  show that these cured resins have a rubberlike region. Table III summarizes the temperatures of  $\alpha$ - and  $\beta$ -transitions, and  $\tan \delta_{\max}$  of all the cured resins examined. The  $T_g$  determined by the dynamic mechanical properties increased with increase in the ABA(M) content in the feed, being 8° ~ 21°C higher than the HDT.

In the previous paper,<sup>3</sup> the HDT of the metal-containing cured resins obtained by crosslinking BADG with ABA(M)-MDA decreased with increase in the metal content, while the  $T_g$  determined by dynamic mechanical properties was not influenced by the metal content. This difference between HDT and  $T_g$  was attributed to the difference of the determination methods. The HDT would depend on the proportion of each chemical structure existing

in the cured resin sample, and the  $T_g$  is a temperature of relaxation of the main crosslinked part. That is, the metal-containing amine-cured epoxy resins were composed of the main crosslinked structure part and linear chain structure part.<sup>3</sup> Meanwhile, for the metal-containing epoxy resins cured with ABA(M) and dicarboxylic acid anhydride, good correlation between HDT and  $T_g$  was observed<sup>4</sup>; it was suggested that the cured resins have a uniform crosslinked structure. Therefore, the good correlation between HDT and  $T_g$  of the cured resins obtained in the present study suggests that the cured resins have a uniform crosslinked structure.

Cuddihy and Moacanin<sup>7</sup> investigated the dynamic mechanical properties of epoxy resins cured with various curing agents; they estimated that the  $\beta$  relaxation is attributable to the local mode of bisphenol A skeleton and to neighboring mobile structure parts. Similarly, Ochi et al.<sup>8</sup> reported that the  $\beta$  relaxation of the amine-cured epoxy resins is attributable to the mobile structure parts such as the hydroxy ether structure and the local mode of bisphenol A skeleton, and the  $\beta$  relaxation shifts to higher temperature with an increase in the amount of hydroxy ether structure. Further, Ochi et al.<sup>9</sup> investigated dynamic mechanical properties of methoxy group and spiro-ring-containing epoxy resins cured with MDA; they found that the  $\beta$  relaxations shifted to lower temperature and became small with a decrease in the produced hydroxy ether structure content.

Therefore, the  $\beta$  relaxation in the present study is inferred to be attributable to the local mode of

**Table IV Boiling Water Resistance of Cured Resins**

| Components            | Mole Ratio of Components | Change in Length (%) | Change in Thickness (%) | Change in Weight (%) | External Appearance <sup>b</sup> |
|-----------------------|--------------------------|----------------------|-------------------------|----------------------|----------------------------------|
| MDA-BADG <sup>a</sup> | 1 : 40                   | 0.07                 | 0.27                    | 0.52                 | UA                               |
|                       | 1 : 20                   | 0.19                 | 0.20                    | 0.54                 | UA                               |
|                       | 1 : 13.3                 | 0.17                 | 0.36                    | 0.51                 | UA                               |
|                       | 1 : 10                   | 0.12                 | 0.17                    | 0.49                 | UA                               |
| ABA (Mg)-BADG         | 1 : 40                   | 0.30                 | 0.19                    | 0.84                 | UA                               |
|                       | 1 : 20                   | 0.18                 | 0.32                    | 0.78                 | UA                               |
|                       | 1 : 13.3                 | 0.07                 | 0.50                    | 0.87                 | UA                               |
|                       | 1 : 10                   | 0.05                 | 0.37                    | 0.87                 | UA                               |
| ABA (Ca)-BADG         | 1 : 40                   | 0.33                 | 0.23                    | 0.75                 | UA                               |
|                       | 1 : 20                   | 0.27                 | 0.31                    | 0.84                 | UA                               |
|                       | 1 : 13.3                 | 0.26                 | 0.50                    | 0.99                 | UA                               |

<sup>a</sup> DMBA was added as a catalyst at a concentration of 2.0 wt % based on the total weight of reactants.

<sup>b</sup> UA = unaffected.

bisphenol A skeleton and to neighboring mobile structures such as the hydroxy ether structure.

The  $\beta$  relaxation appeared at room temperature in the cured resins with high ABA(Mg) content. Though not shown here, the  $\beta$  relaxation was also observed for the MDA or ABA(Ca)-containing cured resin. However, it is not clear whether the  $\beta$  relaxation is based on the  $>N-C_6H_4-CH_2-C_6H_4-N<$  or  $>N-C_6H_4-COOMOOC-C_6H_4-N<$  structure part of the aromatic amines or on another crosslinked structure part.

### Thermal Properties

Figure 9 shows the TGA and DTA curves of the cured resins. The cured resin of MDA-BADG (1 : 10) exhibited thermal decomposition which can be divided into the following four stages: The first stage is a region of ca. 280°–350°C, where abrupt weight loss of ca. 40% occurs with a medium exotherm. The second is a region of ca. 350°–470°C, where slow decomposition occurs. The third is a region of ca. 470°C, where again rapid weight loss of ca. 20% occurs with a large exotherm. The fourth is a region above ca. 470°C, where slow weight loss of ca. 10% occurs.

On the other hand, the Ca-containing cured resin showed thermal decomposition which can be divided into the following two stages: The first stage is a region of ca. 270°–350°C, where abrupt weight loss of ca. 95% occurs with a large exotherm. The second is a region above ca. 350°C, where very slow weight loss occurs with a slight exotherm.

The Mg-containing cured resin showed thermal decomposition which can be divided into the follow-

ing four stages: The first stage is a region of ca. 270°–350°C, where abrupt weight loss of ca. 40% occurs with a medium exotherm. The second is a region of ca. 350°–410°C, where slow decomposition occurs. The third is a region of ca. 410°C, where again rapid weight loss of ca. 40% occurs with a large exotherm. The fourth is a region above ca. 410°C, where slow weight loss occurs. The third decomposition of the metal-containing cured resin occurs at lower temperature than that of the MDA-based resin. It is suggested that the metal carboxylate groups act as a catalyst for the thermal decomposition.

Furthermore, the plateau observed above ca. 500°C in the TGA curves of the metal-containing cured resins corresponds to the formation of MgO for the Mg salt and CaCO<sub>3</sub> for the Ca salt.

### Boiling Water and Water Resistances

Table IV shows the boiling water resistance of the cured resins. The boiling water resistance was evaluated by weight gain, change in dimension, and external appearance by immersion in boiling water for 2 h. The weight gains of the metal-containing cured resins were only slightly higher than those of the resins without metal at the same mole ratios of components; however, the weight gains of all the resins were below 1%. Further, they showed small change in dimension and did not show any change in external appearance.

Figure 10 shows the water absorption of the cured resins at 23°C. In general, the weight gain from water absorption was slightly higher for the metal-containing cured resins than for the resins without metal. However, all the resins showed small weight

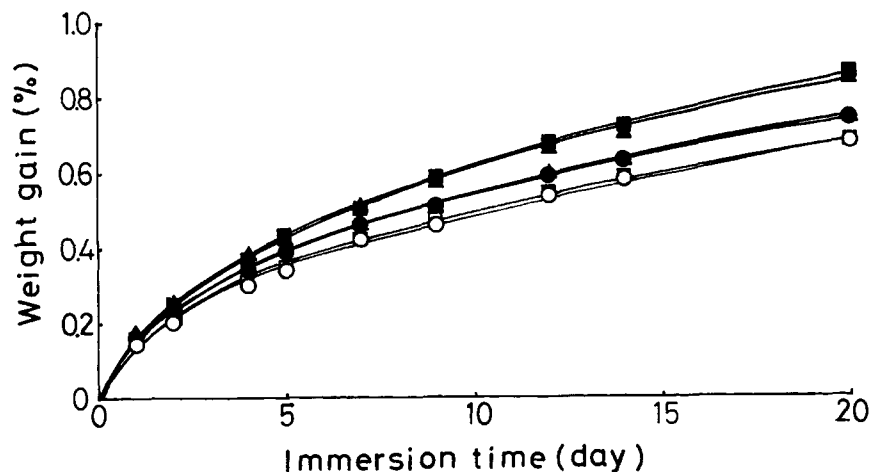


**Figure 10** Effect of water on weight gain of cured resins. (O) MDA-BADG (1 : 40); (●) MDA-BADG (1 : 13.3); (□) ABA(Mg)-BADG (1 : 40); (■) ABA(Mg)-BADG (1 : 13.3); (Δ) ABA(Ca)-BADG (1 : 40); (▲) ABA(Ca)-BADG (1 : 13.3).

gains of below 1% after water immersion at 23°C for 20 days. Their external appearance did not change.

In summary, the metal-containing cured resins in the present study have high boiling water and water resistances.

## REFERENCES

1. H. Matsuda and S. Takechi, *J. Polym. Sci., Part A: Polym. Chem.*, **28**, 1895 (1990).
2. H. Matsuda and S. Takechi, *J. Polym. Sci., Part A: Polym. Chem.*, **29**, 83 (1991).
3. S. Takechi and H. Matsuda, *J. Appl. Polym. Sci.*, **48**, 1105 (1993).
4. S. Takechi and H. Matsuda, *J. Appl. Polym. Sci.*, **51**, 537 (1994).
5. C. C. Price and D. D. Carmelite, *J. Am. Chem. Soc.*, **88**, 4039 (1966).
6. Y. Tanaka, M. Tomoi, and H. Kakiuchi, *J. Macromol. Sci., A-1*, **3**, 471 (1967).
7. E. F. Cuddihy and J. Moacanin, *J. Polym. Sci., A-2*, **8**, 1627 (1970).
8. K. Ochi, T. Takahama, and M. Shimbo, *Nippon Kagaku Kaishi*, **5**, 662 (1979).
9. K. Ochi, M. Yoshizumi, and M. Shimbo, *J. Polym. Sci., Part B: Polym. Phys. Ed.*, **25**, 1817 (1987).

Received January 31, 1994

Accepted July 1, 1994